IEEE Access
Multidisciplinary | Rapid Review | Open Access Journal

Received 19 May 2026, accepted 8 June 2026, date of publication 10 June 2026, date of current version 16 June 2026.

Digital Object Identifier 10.1109/ACCESS.2026.3702536

RESEARCH ARTICLE

Stability Analysis of Control Systems With First-Order Reset Elements, a Frequency-Domain Approach

ALI HOSSEINI AND HASSAN HOSSEINNIA, (Senior Member, IEEE)
Department of Precision and Microsystems Engineering, Delft University of Technology, 2628 CD Delft, The Netherlands

Corresponding author: Ali Hosseini (S.A.Hosseini@tudelft.nl)

This work was supported by ASMPT and Holland High Tech, Topsector High Tech Systems and Materials, with a PPS Innovation Grant Public-Private Collaboration for Research and Development.

ABSTRACT Reset control systems (RCSs) can achieve performance beyond that of conventional linear time-invariant (LTI) controllers, while also allowing analysis directly in the frequency domain using measured frequency response functions (FRFs). Despite this potential, existing frequency-domain stability approaches are typically restricted to specific RCS architectures and commonly depend on parametric plant models, which limits their applicability in practice. In this paper, a generalized H_β framework is developed for the most comprehensive class of RCS structures, incorporating pre-, post-, and parallel LTI filters, as well as nonzero after-reset values. Based on this formulation, an FRF-based representation corresponding to the H_β transfer function is derived, and frequency-domain sufficient conditions are established to certify the H_β-based quadratic stability criterion. As a result, the proposed framework enables direct FRF-based assessment of quadratic stability and convergence for the considered class of reset control systems, using the measured plant FRF together with the known controller and filter transfer functions, without requiring an explicit parametric plant model. The effectiveness and practical relevance of the method are demonstrated through an illustrative industrial case study.

INDEX TERMS Data-based stability analysis, frequency domain analysis, precision motion systems, quadratic stability, reset control systems.

I. INTRODUCTION

Reset elements are nonlinear filters used to overcome the fundamental limitations of linear time-invariant (LTI) control systems [1]. The Clegg integrator (CI) [2] and the generalized first-order reset element (GFORE) [3] are two commonly used reset elements. Both were revisited in [4], and their stability and performance were analyzed in [5]. One major advantage of reset elements over other nonlinear elements is that their behavior can be characterized in the frequency domain even under closed-loop conditions [6]. This feature enables controller design without requiring a parametric plant model, since a measured frequency response function (FRF) can be directly employed.

The associate editor coordinating the review of this manuscript and approving it for publication was Xueguang Zhang.

In this regard, several frequency-domain stability analysis methods have been proposed for reset control systems (RCSs). In [7], a frequency-domain stability analysis method was developed based on the input–output behavior of RCSs. Although this framework can address certain parallel interconnections, its applicability relies on the reset element satisfying a prescribed sector bound. In [8], the authors approximate the scaled graph of reset controllers and provide a graphical tool for assessing the stability of RCSs under a specific reset-action condition. However, the connection of this approach to an explicit FRF-based representation for zero-crossing reset systems is not direct. In [9], the H_β method was introduced to assess the quadratic stability of an RCS. The conventional H_β approach still relies on a parametric model in order to determine both a positive-definite matrix and a vector defining the output

of a transfer function that must be strictly positive real. Moreover, the formulation in [9] is limited to RCSs in which the error is the reset-triggering signal and no prefiltering of the reset element is allowed. The same limitations apply to [10] and [11]. Similarly, the FRF-based H_β-related method in [12] is restricted to series RCS architectures and does not directly apply to the parallel reset structure considered in this paper.

To the best of the authors' knowledge, no H_β-based result is currently available for an RCS that simultaneously: 1) has the architecture shown in Fig. 1, including pre-, post-, and parallel LTI filters together with a shaping filter, and 2) allows a nonzero after-reset value (γ, introduced later). Therefore, the conventional matrix-based H_β framework must be extended to accommodate this more general class of reset control systems. Following the framework proposed in [11], this study, in Theorem 1,

- extends the H_β method to the general RCS architecture shown in Fig. 1, including nonzero after-reset values.

In [12], FRF-based conditions related to the matrix-form H_β criterion were presented. Although an FRF-based transfer function was derived, the formulation remained largely intuitive and lacked a formal mathematical connection to the model-based H_β representation. Furthermore, the method is restricted to series RCS architectures without an LTI element in parallel with the reset element, and therefore does not apply to systems with a feedthrough term. Compared with other frequency-domain tools, such as the sector-bound method in [7] and the scaled-graph method in [8], the proposed approach targets a different certificate, namely H_β-based quadratic stability, while allowing the general architecture in Fig. 1, including pre-, post-, parallel, and shaping filters. Moreover, the reset element is not restricted to sector-bound reset behavior or to specific reset-action conditions. Therefore, the proposed criterion is less restrictive regarding the admissible architecture, the reset-triggering condition, and the need for a parametric plant model. However, it remains a frequency-domain-based condition and is not claimed to be uniformly less conservative across all reset systems. Since satisfaction of the H_β-based quadratic stability conditions is needed in order to employ the uniformly exponential convergence tools in [13], a gap remains in the FRF-based assessment of convergence for non-series RCSs. To address this gap, this study, in Lemma 4,

- derives an FRF-based representation corresponding to the model-based H_β transfer function;

and then, in Theorem 2,

- establishes frequency-domain conditions that are sufficient to verify the H_β-based quadratic stability criterion.

These developments make it possible to assess the quadratic stability and convergence of RCSs with architectures such as that shown in Fig. 1, including cases with nonzero after-reset values. It should be emphasized that the proposed method is plant-model-free in the sense that no parametric model of $G(s)$ is required; the remaining LTI

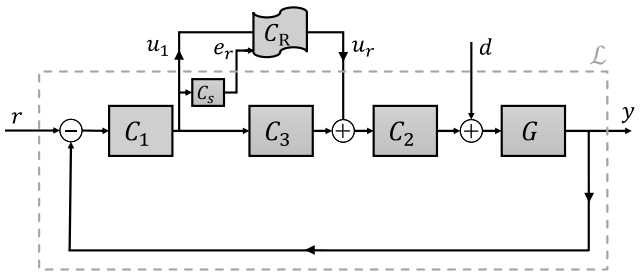

FIGURE 1. The closed-loop architecture of a reset control system.

controller and filter blocks, namely $C_1(s)$, $C_2(s)$, $C_3(s)$, and $C_s(s)$, are assumed to be known from the controller design.

The ability to analyze the stability and convergence of the system structure in Fig. 1 is particularly important because parallel reset architectures have shown significant potential in several studies [14], [15]. Nevertheless, the lack of a stability-assessment framework for this class of systems has two major consequences. First, the stability properties of such systems remain unknown. Second, and more importantly, the absence of stability and convergence guarantees prevents the application of closed-loop frequency-domain design methods developed for reset control systems [6], [16]. Consequently, designers are constrained to a limited set of reset-control architectures for which such frequency-domain tools are available.

The remainder of this paper is organized as follows. Section II describes the closed-loop RCS and recalls the main theorems and lemmas used throughout the paper. Section III presents the main results. The utility of the proposed approach is illustrated through the example in Section IV. Finally, conclusions and directions for future work are given in Section V.

II. PRELIMINARIES

A. SYSTEM DESCRIPTION

In the following, we provide an introduction to the RCS and demonstrate its parallel interconnection with an LTI system, resulting in a SISO closed-loop system, as depicted in Fig. 1. The linear part contains G as the plant; C_1, C_2, and C_3 as the linear controllers; and a shaping filter C_s. Additionally, C_R serves as the first-order reset element, presented as:

$$C_R : \begin{cases} \dot{x}_r(t) = A_r x_r(t) + B_r u_1(t), & x_r(t) \notin \mathcal{K}, \\ x_r(t^+) = \gamma x_r(t), & x_r(t) \in \mathcal{K}, \\ u_r(t) = C_r x_r(t) + D_r u_1(t). \end{cases} \tag{1}$$

where $A_r \in \mathbb{R}$, $B_r \in \mathbb{R}$, $C_r \in \mathbb{R}$, and $D_r \in \mathbb{R}$ represent the state-space matrices of the reset element. $x_r(t) \in \mathbb{R}$ is the state of the reset element, $x_r(t^+) \in \mathbb{R}$ is the post-reset state, $u_1(t) \in \mathbb{R}$ and $u_r(t) \in \mathbb{R}$ represent the input and output of the reset element, respectively. The reset surface is defined as

$$\mathcal{K} := \left\{ (x_r, e_r) \in \mathbb{R}^2 : e_r = 0 \ \wedge \ |(1-\gamma)x_r| \geq \delta \right\}, \tag{2}$$

where $\gamma \in \mathbb{R}$ is the post-reset state coefficient and δ is a small positive constant that excludes trivial or arbitrarily small reset jumps. $e_r(t)$ is the output of the shaping filter C_s.

In this study, C_R is considered to be a first-order reset element (CI or GFORE). By considering $C_r B_r = \omega_k \in \mathbb{R}^{>0}$ and $A_r = -\omega_r$ ($\omega_r \in \mathbb{R}^{\geq 0}$), the general form of the reset element used in this paper is defined, and its base linear transfer function (no reset action) is as follows

$$R(s) = C_r(s - A_r)^{-1}B_r + D_r = \frac{\omega_k}{s + \omega_r} + D_r, \tag{3}$$

where $s \in \mathbb{C}$ is the Laplace variable. The reset element represents a CI or proportional CI when $\omega_r = 0$ and represents a GFORE element when $\omega_r \neq 0$.

For the LTI part of the closed-loop system, which is denoted by $\mathcal{L}$, we have

$$\mathcal{L}: \begin{cases} \dot{x}_l(t) = Ax_l(t) + B_u u_r(t) + Bw(t), \\ y(t) = Cx_l(t), \\ u_1(t) = C_u x_l(t) + D_u w(t), \\ e_r(t) = C_e x_l(t) + D_e w(t), \end{cases} \tag{4}$$

where $x_l(t) \in \mathbb{R}^{n_l}$ is the state of the LTI part of the system, and $w(t) = \begin{bmatrix} r(t) & d(t) \end{bmatrix}^T \in \mathbb{R}^2$, in which $r(t)$ and $d(t)$ are the reference and disturbance signals, respectively. Also, $A \in \mathbb{R}^{n_l \times n_l}$, $B \in \mathbb{R}^{n_l \times 2}$, $C \in \mathbb{R}^{1 \times n_l}$, $B_u \in \mathbb{R}^{n_l \times 1}$, $C_u \in \mathbb{R}^{1 \times n_l}$, $D_u \in \mathbb{R}^{1 \times 2}$, $C_e \in \mathbb{R}^{1 \times n_l}$ and $D_e \in \mathbb{R}^{1 \times 2}$ are the corresponding dynamic matrices. The matrices in (4) realize the LTI interconnection in Fig. 1, excluding C_R. Thus, A contains the dynamics of G, C_1, C_2, C_3, and C_s, while B_u, C_u, and C_e define the channels from u_r to the LTI subsystem, from the LTI state to u_1, and from the LTI state to e_r, respectively. This realization satisfies

$$\begin{aligned} C_u(sI - A)^{-1}B_u &= -\frac{L(s)}{1 + L(s)C_3(s)}, \\ C_e(sI - A)^{-1}B_u &= -\frac{L(s)C_s(s)}{1 + L(s)C_3(s)}, \end{aligned} \tag{5}$$

with $L(s) = C_1(s)C_2(s)G(s)$.

Assumption 1: In this study, it is assumed that there is no direct feedthrough from input $w(t)$ and $u_r(t)$ to plant output $y(t)$ and from $u_r(t)$ to $u_1(t)$ and $e_r(t)$.

Assumption 1 is reasonable, as it pertains to any causal LTI element C_1, C_2, C_3, and any plant G with a relative degree greater than zero, which includes the vast majority of motion and mass-based systems. Hence, the closed-loop state-space representation of the overall RCS can be expressed as follows

$$\text{RCS}: \begin{cases} \dot{x}(t) = \bar{A}x(t) + \bar{B}w(t), & x(t) \notin \mathcal{F}_\delta, \\ x(t^+) = A_\rho x(t), & x(t) \in \mathcal{F}_\delta, \\ e_r(t) = \bar{C}_e x(t) + \bar{D}_e w(t), \\ y(t) = \bar{C}x(t), \end{cases} \tag{6}$$

in which $x(t) = \begin{bmatrix} x_r(t)^T & x_l(t)^T \end{bmatrix}^T \in \mathbb{R}^{1+n_l}$, $\bar{C} = \begin{bmatrix} 0 & C \end{bmatrix}$, $\bar{B} = \begin{bmatrix} 0_{1\times 2} \\ B \end{bmatrix} + \begin{bmatrix} B_r D_u & 0_{1\times 1} \\ B_u D_r D_u & 0_{n_l \times 1} \end{bmatrix}$, $\bar{A} = \begin{bmatrix} A_r & B_r C_u \\ B_u C_r & A + B_u D_r C_u \end{bmatrix}$, $A_\rho = \begin{bmatrix} \gamma & 0_{1\times n_l} \\ 0_{n_l \times 1} & I_{n_l \times n_l} \end{bmatrix}$, and $\bar{C}_e = \begin{bmatrix} 0 & C_e \end{bmatrix}$. With the reset surface

$$\mathcal{F}_\delta := \left\{ x \in \mathbb{R}^{n_l+1} : \bar{C}_e x + \bar{D}_e w = 0, \ \|(I - A_\rho)x\| \geq \delta \right\}. \tag{7}$$

The following remark further discusses the proposed reset surface.

Remark 1: To avoid the well-posedness issue associated with the reset set defined through a strict inequality, the reset surface presented in [9]

$$\mathcal{M} = \{x : C_{\text{cl}}x = 0, \ (I - A_R)x \neq 0\}, \tag{8}$$

is regularized in this study as

$$\mathcal{F}_\delta := \left\{ x \in \mathbb{R}^{n_l+1} : \bar{C}_e x + \bar{D}_e w = 0, \ \|(I - A_\rho)x\| \geq \delta \right\}. \tag{9}$$

That is, resets are allowed only when the reset signal is zero, and the corresponding jump is nontrivial. This modification preserves the original reset law $x^+ = A_\rho x$ and only excludes ineffective reset events for which the jump amplitude is arbitrarily small. This regularization is motivated by Remark 1 in [17], where it is pointed out that reset models based on a set of the form of (8) may suffer from two related issues: first, solutions may be ambiguous at points satisfying $C_{\text{cl}}x = 0$ and $(I - A_R)x = 0$; second, the reset set is not closed because of the condition $(I - A_R)x \neq 0$. The modified set $\mathcal{F}_\delta$ removes this defect by replacing the strict inequality with the closed condition $\|(I - A_\rho)x\| \geq \delta$, and therefore excludes exactly the class of degenerate points responsible for the above ambiguity.

At the same time, the quadratic-stability argument (discussed in the next section) is preserved exactly for the regularized model. Indeed, the Lyapunov decrease condition along flows is unchanged, while the jump condition is verified on the admissible reset set F_δ, which is a subset of the nontrivial-jump set of the unregularized model. Hence, the regularization does not approximate the stability proof itself; rather, it modifies the reset law in a way that yields a well-posed system. For sufficiently small δ, the regularized model approaches the original reset law away from degenerate reset points.

B. FOUNDATIONAL THEOREMS AND LEMMAS

This section presents the fundamental results that underpin the remainder of the study. As discussed earlier, the analysis in this work is based on the H_β stability framework. The H_β condition relies on the existence of a quadratic Lyapunov function that decreases along the flow dynamics over the entire state space and is non-increasing across reset jumps. This approach was originally introduced in [9] for the cases with the reset surface defined as (8) and $\gamma = 0$, as also reported in [11, Chapter 4.4]. In the present work, however, the reset surface is denoted by $\mathcal{F}_\delta$, nonzero values of γ are also considered, and the RCS includes two additional filters, namely a prefilter C_1 and a parallel filter C_3. Therefore, the H_β framework is extended here to assess the quadratic stability of the RCS in (6).

Before presenting the quadratic stability theorem, the following lemma recalls the strictly positive realness (SPR) conditions used throughout the analysis.

Lemma 1: [18, Lemma 6.1], Let $H(s)$ be a proper rational $p \times p$ transfer function and assume $\det[H(s) + H^T(-s)]$ is not identically zero. Then, $H(s)$ is SPR if and only if:

- $H(s)$ is Hurwitz,
- $H(j\omega) + H^T(-j\omega)$ is positive definite for all $\omega \in \mathbb{R}$,
- either $H(\infty) + H^T(\infty)$ is positive definite or if $H(\infty) + H^T(\infty)$ is positive semi-definite, $\lim_{\omega\to\infty} \omega^2 M^T [H(j\omega) + H^T(-j\omega)]M > 0$, for any $p(p-q)$ full rank matrix M such that $M^T[H(\infty) + H^T(\infty)]M = 0$, and $q = \text{rank}[H(\infty) + H^T(\infty)]$.

Using Lemma 1, the following theorem establishes a sufficient condition for the quadratic stability of the reset control system (6).

Theorem 1: The zero equilibrium of the reset control system (6) with $w = 0$ is quadratically stable if there exist $\varrho > 0$ and $\beta \in \mathbb{R}$ such that the transfer function

$$H_\beta(s) = C_0(sI - \bar{A})^{-1}B_0, \tag{10}$$

with

$$C_0 = \begin{bmatrix} \varrho & \beta C_e \end{bmatrix}, \quad B_0 = \begin{bmatrix} 1 \\ 0_{n_l \times 1} \end{bmatrix}, \tag{11}$$

is SPR, $(\bar{A}, B_0)$ and $(\bar{A}, C_0)$ are controllable and observable respectively, and $-1 \le \gamma \le 1$.

The proof of Theorem 1 is provided in Appendix A, following the approach used in [11, Proposition 4.5].

By applying Theorem 1, the quadratic stability of an RCS can be evaluated under zero-input conditions. However, in nearly all frequency-domain analyses of closed-loop RCSs [6], it is also important to demonstrate the convergence of the closed-loop system in response to specific non-zero inputs. Therefore, the following lemma is recalled from [13, Lemma 2].

Lemma 2: [13, Lemma 2], The reset control system in (6) is uniformly exponentially convergent [19, Definition 2] for any input w that qualifies as a Bohl function, if

- There are infinitely reset instants t_k ($t_k \in R \ge 0, k \in \mathbb{N}$), and $\lim_{k\to\infty} t_k = \infty$;
- All conditions in Theorem 1 hold;
- The initial condition of the reset element is zero.

Since the convergence of RCSs has been established for Bohl function inputs, note that step, ramp, and sinusoidal functions all belong to the class of Bohl functions [20, Theorem 2.7]. Please also note that although the proof of Lemma 2 in [13] is given for a class of RCSs without a parallel path and shaping filter ($C_3 = 0$ and $C_s = 1$), it remains identical for the RCS in this study, as [13] decomposes the closed-loop dynamics into linear and nonlinear parts like in Fig. 1.

Finally, the following lemma is introduced to facilitate the derivation of the FRF-based H_β transfer function in the next section.

Lemma 3: [Woodbury matrix identity] [21, Appendix. A,Prob. 13.9]

Let K, U, J, and V be matrices of compatible dimensions. Then

$$\begin{aligned}&(K + UJV)^{-1} \\ &= K^{-1} - K^{-1}U(J^{-1} + VK^{-1}U)^{-1}VK^{-1}.\end{aligned} \tag{12}$$

III. FRF BASED H_β METHOD

In this section, an equivalent FRF–based form of $H_\beta(s)$ is derived from the model-based expression in (10). The corresponding quadratic stability conditions of Theorem 1 are then reformulated in Theorem 2, enabling the use of Lemma 2 to assess RCSs' convergence without a parametric system model.

Lemma 4: Under Assumption 1, the transfer function in (10) can be rewritten as follows

$$H_\beta(s) = \frac{\beta' L(s)C_s(s)\Big(R(s)-D_r\Big) + \varrho'\Big(1+L(s)\Big(C_3(s)+D_r\Big)\Big)\Big(R(s)-D_r\Big)}{1+L(s)\Big(R(s)+C_3(s)\Big)}, \tag{13}$$

where $L(s) = C_1(s)C_2(s)G(s)$, $\beta' = \frac{-\beta}{B_r}$, and $\varrho' = \frac{\varrho}{C_r B_r}$, which $B_r \in \mathbb{R}$ and $C_r \in \mathbb{R}$ are the input and output matrix of the reset element C_R with $B_r C_r > 0$.

Proof: Appendix B

Lemma 4 rewrites $H_\beta(s)$ in terms of the frequency-domain quantities $L(s)$, $C_s(s)$, $C_3(s)$, and $R(s)$. As a result, the quadratic-stability condition in Theorem 1 can be examined without explicitly constructing the state-space matrices of the overall closed-loop system. This representation forms the basis for the frequency-domain stability criterion developed next. First, we introduce three definitions that will be used in Theorem 2.

Definition 1: For the transfer function in (13), the Nyquist Stability Vector (NSV) is defined as ($\forall\, \omega \in \mathbb{R}$)

$$\begin{aligned}\vec{\mathcal{N}}(\omega) &= \begin{bmatrix}\mathcal{N}_x(\omega) & \mathcal{N}_y(\omega)\end{bmatrix}^T \\ &= \begin{bmatrix}\Re(M_1^*(j\omega)M_2(j\omega)) & \Re(M_1^*(j\omega)M_3(j\omega))\end{bmatrix}^T,\end{aligned} \tag{14}$$

where $\Re(.)$ means the real part, $(.)^*$ means the complex conjugate, $j^2 = -1$, and

$$\begin{aligned}M_1(j\omega) &= 1 + L(j\omega)\Big(R(j\omega) + C_3(j\omega)\Big), \\ M_2(j\omega) &= L(j\omega)C_s(j\omega)\Big(R(j\omega) - D_r\Big), \\ M_3(j\omega) &= \Big(1 + L(j\omega)\Big(C_3(j\omega) + D_r\Big)\Big)\Big(R(j\omega) - D_r\Big).\end{aligned} \tag{15}$$

Definition 2: For the Nyquist Stability Vector $\vec{\mathcal{N}}(\omega) = \begin{bmatrix}\mathcal{N}_x(\omega) & \mathcal{N}_y(\omega)\end{bmatrix}^\top$, define its phase as

$$\theta_{\mathcal{N}}(\omega) := \angle\vec{\mathcal{N}}(\omega) := \text{atan2}\Big(\mathcal{N}_y(\omega),\, \mathcal{N}_x(\omega)\Big), \quad \forall\, \omega \in \mathbb{R}. \tag{16}$$

Moreover, define

$$\theta_1 := \min_{\omega\in\mathbb{R}} \theta_{\mathcal{N}}(\omega), \qquad \theta_2 := \max_{\omega\in\mathbb{R}} \theta_{\mathcal{N}}(\omega). \tag{17}$$

In this paper, for simplicity, the phase is taken in the interval

$$\theta_{\mathcal{N}}(\omega) \in \left[-\frac{\pi}{2}, \frac{3\pi}{2}\right).$$

Definition 3: The transfer function $L(s)C_s(s)$ is defined as

$$L(s)C_s(s) = \frac{K_m s^m + K_{m-1}s^{m-1} + \ldots + K_{m_0}}{K_n s^n + K_{n-1}s^{n-1} + \ldots + K_{n_0}}. \tag{18}$$

To enable the application of Lemma 2 in the frequency domain, the conditions of Theorem 1 are next translated into verifiable frequency-domain conditions. Based on the preceding lemmas and definitions, Theorem 2 reformulates the H_β-based quadratic stability criterion in Theorem 1 into verifiable frequency-domain conditions.

Theorem 2: Consider the reset control system (6) under Assumption 1, with $w(t) = 0$. If all the conditions listed below are satisfied, then the conditions of Theorem 1 hold. Consequently, the zero equilibrium of the reset control system (6) is quadratically stable.

- The base linear system is asymptotically stable, and its open-loop transfer function does not have any unstable pole-zero cancellation. Also, the shaping filter $C_s(s)$ is asymptotically stable.
- $-1 \leq \gamma \leq 1$.
- $B_r C_r > 0$.
- $(\theta_2 - \theta_1) < \pi$.

In the case of $\omega_r \neq 0$ (GFORE), at least one of the following two conditions must hold:

- $-\frac{\pi}{2} < \theta_N(\omega) < \pi, \forall \omega \in [0, \infty)$;
- $0 < \theta_N(\omega) < \frac{3\pi}{2}, \forall \omega \in [0, \infty)$.

In the case of $\omega_r = 0$ (CI)

- The relative degree of $L(s)C_s(s)$ must be 1.
- If $\lim_{s\to\infty} \angle\,(L(s)C_s(s)) = -\pi/2$ ($\frac{K_n}{K_m} > 0$), then $0 < \theta_{\mathcal{N}}(\omega) < \frac{3\pi}{2}\ \forall \omega \in [0, \infty)$.
- If $\lim_{s\to\infty} \angle\,(L(s)C_s(s)) = -3\pi/2$ ($\frac{K_n}{K_m} < 0$), then $-\frac{\pi}{2} < \theta_{\mathcal{N}}(\omega) < \pi, \forall \omega \in [0, \infty)$.

Proof: Appendix C

Using Theorem 2, we can now assess the quadratic stability of the RCS in (6) based solely on the measured FRF of the plant. This, in turn, enables the application of Lemma 2 to the frequency-domain convergence assessment of RCSs, as stated in the following corollary.

Corollary 1: Suppose that w is a Bohl function, the initial condition of the reset element C_R is zero, and all conditions in Theorem 2 hold. Then, the reset control system (6) is uniformly exponentially convergent if either the reset instants are infinite and unbounded, i.e., $t_k \to \infty$ as $k \to \infty$, or the reset sequence is finite.

Proof: If the reset instants are infinite and unbounded, the result follows directly from Lemma 2. If the reset sequence is finite, then there exists a finite time $T_f \geq 0$ such that no reset occurs for all $t \geq T_f$, i.e., the reset surface F_δ is no longer reached. Hence, after T_f, the jump map is no longer invoked and the system evolves according to the base linear closed-loop dynamics. Since Theorem 2 requires the base linear system to be asymptotically stable, the difference between any two solutions driven by the same Bohl input decays exponentially for all $t \geq T_f$. Therefore, convergence follows either from Lemma 2 in the infinite-reset case or from the asymptotic stability of the base linear system in the finite-reset case. ■

IV. ILLUSTRATIVE EXAMPLES

In this section, the proposed method is applied to analyze the stability of an industrial precision positioning stage in an ASMPT wire-bonding machine. A wire bonder is a machine used to connect conducting wires between an integrated circuit and its package, thereby forming a microchip. The isolated XYZ motion stage of the wire bonder is depicted in Fig. 2. Accordingly, the measured FRF of the X-stage, from actuator force (F_x) to displacement in the X-direction (D_x), is illustrated in Fig. 2b. To preserve confidentiality, the frequency axis has been normalized. To facilitate interpretation of the frequency response, the sampling frequency of the setup can be considered to be on the order of 10 kHz. The LTI controller C_{L} is adopted from [14] and is augmented with three add-on reset-based controllers. The reset controller C_{R_1} is considered as

$$\begin{aligned} C_R = \mathrm{GFORE}\big(&A_r = -\omega_r, B_r = 1, C_r = \omega_r, D_r = 1,\\ &\gamma = 0\big),\ C_s(s) = 1,\ C_1(s) = \frac{1 + s/(Q_1\omega_n) + s^2/\omega_n^2}{1 + s/(Q_2\omega_n) + s^2/\omega_n^2},\\ C_2(s) = C_{\mathrm{L}}k_c&\left(\frac{1 + s/\omega_l}{1 + s/\omega_f}\right),\ \text{and}\ C_3(s) = 0. \end{aligned} \tag{19}$$

The reset controller C_{R_2} is considered as

$$\begin{aligned} C_R = \mathrm{GFORE}\big(&A_r = -\omega_r, B_r = 1, C_r = \omega_r, D_r = -0.41,\\ &\gamma = -0.1\big),\ C_s(s) = \frac{1 + s/\omega_1}{1 + s/\omega_2},\\ C_1(s) = \frac{1 + s/(Q_1\omega_n) + s^2/\omega_n^2}{1 + s/(Q_2\omega_n) + s^2/\omega_n^2},&\\ C_2(s) = C_{\mathrm{L}}k_c&\left(\frac{1 + s/\omega_l}{1 + s/\omega_f}\right),\ \text{and}\ C_3(s) = \left(\frac{1 + s/\omega_d}{1 + s/\omega_t}\right). \end{aligned} \tag{20}$$

The reset controller C_{R_3} is considered as

$$\begin{aligned} C_R = \mathrm{GFORE}\big(&A_r = -\omega_r, B_r = 1, C_r = \omega_r, D_r = -0.37,\\ &\gamma = 0.1\big),\ C_s(s) = \frac{1 + s/\omega_1 + s^2/\omega_3^2}{1 + s/\omega_2 + s^2/\omega_4^2},\\ C_1(s) = \frac{1 + s/(Q_1\omega_n) + s^2/\omega_n^2}{1 + s/(Q_2\omega_n) + s^2/\omega_n^2},&\\ C_2(s) = C_{\mathrm{L}}k_c&\left(\frac{1 + s/\omega_l}{1 + s/\omega_f}\right),\ \text{and}\ C_3(s) = \left(\frac{1 + s/\omega_d}{1 + s/\omega_t}\right). \end{aligned} \tag{21}$$

The corresponding parameters for each controller are provided in Table 1.

Given the plant shown in Fig. 2b and the controllers in (19), (20), and (21), Theorem 2 is employed to assess the quadratic stability of the corresponding closed-loop systems.

TABLE 1. Controller parameters for C_{R_1}, C_{R_2}, and C_{R_3}, with all frequencies given in rad/s.

Parameter	C_{R_1}	C_{R_2}	C_{R_3}
ω_r	9.70×10^{-2}	5.09×10^{-2}	6.79×10^{-2}
ω_n	4.87×10^{-2}	4.87×10^{-2}	5.65×10^{-2}
ω_l	1.57×10^{-1}	8.25×10^{-2}	1.10×10^{-1}
ω_f	3.14×10^{-1}	1.58×10^{-1}	2.51×10^{-1}
ω_d	–	1.57×10^{-2}	2.75×10^{-2}
ω_t	–	2.36×10^{-2}	3.14×10^{-2}
ω_1	–	3.92×10^{-2}	7.15×10^{-2}
ω_2	–	2.21×10^{-2}	3.48×10^{-2}
ω_3	–	–	6.39×10^{-2}
ω_4	–	–	5.55×10^{-2}
Q_1	1	1.29	0.8
Q_2	4	2.68	4.4
k_c	0.5	0.48	0.56

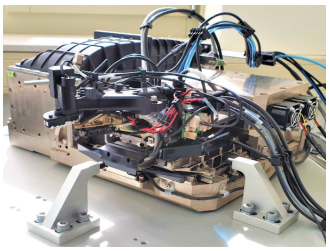

(a)

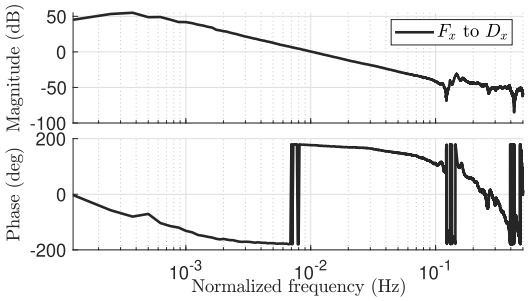

(b)

FIGURE 2. (a) Isolated XYZ motion stage of the wire bonder. (b) FRF of the X-stage, illustrating the mapping of actuator force in the X-stage to the displacement measured by the X-stage encoder.

Since all controllers are designed based on a stable linear base system, with $-1 \leq \gamma \leq 1$ and $B_r C_r > 0$, only the condition on $\theta_{\mathcal{N}}(\omega)$ needs to be verified. Fig. 3 shows $\theta_{\mathcal{N}}(\omega)$ for the three reset controllers. The corresponding values of θ_1, θ_2, and $\theta_2 - \theta_1$ are reported in Table 2. For all considered controllers, $\theta_2 - \theta_1 < \pi$. Moreover, $\theta_{\mathcal{N}}(\omega)$ remains within the admissible GFORE sector $(-\pi/2, \pi)$. Therefore, all closed-loop systems satisfy the NSV condition and are quadratically stable for $w(t) = 0$.

It should be noted, however, that the interpretation of these results in terms of robustness margins is not straightforward. For instance, C_{R_3} yields the largest value of $\theta_2 - \theta_1$, and is therefore closest to violating the admissible sector condition. At the same time, it has the smallest stability margin among the considered controllers in the base-linear design. This may suggest that the stability margins of the

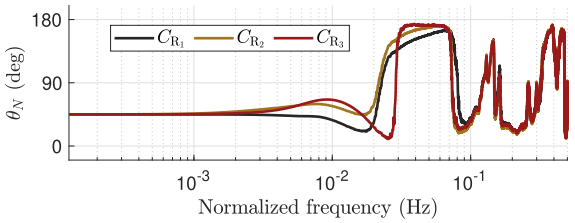

FIGURE 3. $\theta_{\mathcal{N}}(\omega)$ for the controllers C_{R_1}, C_{R_2}, and C_{R_3}.

TABLE 2. Values of θ_1, θ_2, and $\theta_2 - \theta_1$ for the reset controllers.

Controller	θ_1	θ_2	$\theta_2 - \theta_1$
C_{R_1}	12.34°	171.76°	159.42°
C_{R_2}	10.89°	172.69°	161.80°
C_{R_3}	9.97°	173.86°	163.89°

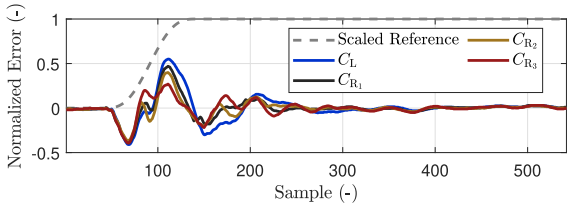

FIGURE 4. Measured error signals for a typical reference trajectory using the designed reset controllers and the nominal LTI controller. The reference trajectory is scaled for visualization.

base-linear dynamics influence the values obtained from the proposed frequency-domain stability assessment. However, this relation is not conclusive. In particular, C_{R_2} is designed to be more robust than C_{R_1} in terms of the base-linear dynamics, for example by providing a larger phase margin. Nevertheless, C_{R_2} results in a larger value of $\theta_2 - \theta_1$, bringing it closer to the boundary of the admissible sector condition. Therefore, although certain trends between the base-linear stability margins and the proposed stability indicators may be observed, the presented method does not directly provide a rigorous quantitative measure of robustness margins.

Furthermore, since the RCSs are designed for zero initial conditions, Corollary 1 implies that each closed-loop system admits a uniformly exponentially convergent solution for any input w that is a Bohl function. This example demonstrates that the stability and convergence properties of an RCS can be assessed even in the absence of a parametric plant model or an explicit transfer function.

Finally, to illustrate the performance and time-domain behavior of the designed reset controllers, the controllers are implemented on the wire bonder and compared with the LTI controller C_L. The corresponding measured error signals are shown in Fig. 4. Please note that, in practice, the reset controller is implemented digitally, so reset decisions are affected by finite sampling time, numerical precision, sensor resolution, quantization, and measurement noise. Therefore, the regularization introduced in Remark 1 is interpreted as an implementation threshold rather than an additional controller

tuning parameter. In this setup, δ is selected above the effective sensor-resolution and noise level, which is on the order of 100 nm, and sufficiently below the typical reset-jump amplitude. Thus, only degenerate or numerically insignificant reset events are excluded, while legitimate reset actions are preserved. The frequency-domain stability test itself is not retuned with δ.

V. CONCLUSION

In this paper, we first extended the existing H_β method to assess the quadratic stability of RCSs with nonzero after-reset values (γ) and general closed-loop architectures. We then analytically established a mapping between the matrix-based H_β transfer function and its FRF-based counterpart. This mapping relaxed the LMI-based conditions and enabled the development of quadratic stability assessment criteria using purely graphical frequency-domain tools. An illustrative example was also provided to demonstrate the assessment of quadratic stability and convergence using the measured FRF of the industrial stage together with the known controller and filter transfer functions. Future work will address robustness analysis and the definition of explicit stability margins for RCSs.

APPENDIX A
PROOF OF THEOREM 1

Using the approach from [11, Proposition 4.5], to demonstrate the quadratic stability of the system in (6), we show the existence of a matrix $P > 0$ such that the quadratic Lyapunov function $V(x(t)) = x^\top(t)Px(t)$ decreases over the entire state space along the system trajectories and is non-increasing at the reset jumps (see [9, Theorem 1]). This leads to the following:

$$\bar{A}^\top P + P\bar{A} < 0, \tag{22}$$

and

$$x^\top(t)\left(A_\rho^\top P A_\rho - P\right)x(t) \le 0,\ \forall x(t) \in \mathcal{F}_\delta, \tag{23}$$

where the reset surface $\mathcal{F}_\delta$ for the zero input case ($w(t) = 0$) gives $\{x(t) \in \mathbb{R}^{n_l+1} : \bar{C}_e x(t) = C_e x_l(t) = 0,\ \|(I - A_\rho)x\| \ge \delta\}$ with $\bar{C}_e = \begin{bmatrix}0 & C_e\end{bmatrix}$.

Considering $P = P^\top = \begin{bmatrix}P_1 & P_2\\ P_2^\top & P_3\end{bmatrix}$, $A_\rho = \begin{bmatrix}\gamma & 0_{1\times n_l}\\ 0_{n_l\times 1} & I_{n_l\times n_l}\end{bmatrix}$, and $x(t) = \begin{bmatrix}x_r(t)^T & x_l(t)^T\end{bmatrix}^T$, for (23) we have:

$$\begin{aligned}&x^\top(t)\left(A_\rho^\top P A_\rho - P\right)x(t)\\ &= (\gamma^2-1)x_r^2(t)P_1 + (\gamma-1)x_r(t)x_l^\top(t)P_2^\top\\ &\quad + (\gamma-1)x_r(t)P_2x_l(t).\end{aligned} \tag{24}$$

By selecting $P_2 = \beta C_e$ where $\beta \in \mathbb{R}$, we have:

$$\begin{aligned}&x^\top(t)\left(A_\rho^\top P A_\rho - P\right)x(t)\\ &= (\gamma^2-1)x_r^2(t)P_1 + (\gamma-1)x_r(t)\beta x_l^\top(t)C_e^\top\\ &\quad + (\gamma-1)x_r(t)\beta C_e x_l(t).\end{aligned} \tag{25}$$

Given that $C_e x_l(t) = 0$ at the reset jumps, the expression simplifies to:

$$x^\top(t)\left(A_\rho^\top P A_\rho - P\right)x(t) = (\gamma^2-1)x_r^2(t)P_1, \tag{26}$$

where for $P_1 > 0$ and $(\gamma^2 - 1) \le 0$ (or $-1 \le \gamma \le 1$) it results

$$x^\top(t)\left(A_\rho^\top P A_\rho - P\right)x(t) \le 0,\ \forall x(t) \in \mathcal{F}_\delta. \tag{27}$$

This implies that the inequality in (23) is satisfied for every $-1 \le \gamma \le 1$ and for matrices $P > 0$ of the form $B_0^\top P = C_0$, where

$$B_0 = \begin{bmatrix}1\\ 0_{n_l\times 1}\end{bmatrix},\quad C_0 = \begin{bmatrix}\varrho & \beta C_e\end{bmatrix}, \tag{28}$$

with $\varrho = P_1 \in \mathbb{R}^+$. Thus, from (22) and $B_0^\top P = C_0$, we can write:

$$\begin{bmatrix}\bar{A}^\top P + P\bar{A} + 2\varepsilon P & PB_0 - C_0^\top\\ B_0^\top P - C_0 & 0\end{bmatrix} \le 0, \tag{29}$$

with $\exists P > 0$ and $\exists \varepsilon > 0$. The remainder of the proof follows that of [11, Proposition 4.5] (from equation (4.30) onward), utilizing the generalized Kalman–Yakubovich–Popov lemma [22]. ■

APPENDIX B
PROOF OF LEMMA 4

Starting from (10), the inverse of $(sI - \bar{A})$ can be written in partitioned form as

$$(sI - \bar{A}) = \begin{bmatrix}s - A_r & -B_rC_u\\ -B_uC_r & sI - A - B_uD_rC_u\end{bmatrix} = \begin{bmatrix}Q_1 & Q_2\\ Q_3 & Q_4\end{bmatrix}. \tag{30}$$

Let $(sI - \bar{A})^{-1} = \begin{bmatrix}W & X\\ Y & Z\end{bmatrix}$. Substituting this in (10) yields

$$H_\beta(s) = \varrho W + \beta C_e Y, \tag{31}$$

so only W and Y are required. Using the standard block-matrix inversion formula [23],

$$W = (Q_1 - Q_2Q_4^{-1}Q_3)^{-1},\qquad Y = -Q_4^{-1}Q_3W. \tag{32}$$

From the block definitions in (30) we have

$$W = \left(s - A_r - B_rC_u(sI - A - B_uD_rC_u)^{-1}B_uC_r\right)^{-1}.$$

Applying the Lemma 3 with $K = s - A_r$, $U = B_rC_u$, and $V = B_uC_r$ gives

$$W = (s-A_r)^{-1} - (s-A_r)^{-1}B_rC_u\Xi^{-1}B_uC_r(s-A_r)^{-1},$$

where $\Xi = -(sI - A) + B_uR(s)C_u$. Having $R(s) = C_r(sI - A_r)^{-1}B_r + D_r$ and using Lemma 3 again, yields

$$\begin{aligned}\Xi^{-1} &= -(sI-A)^{-1}\\ &\quad - (sI-A)^{-1}B_u\left(\frac{R(s)}{1-P(s)R(s)}\right)C_u(sI-A)^{-1},\end{aligned}$$

where from the LTI subsystem (4)

$$P(s) = C_u(sI-A)^{-1}B_u = \frac{-L(s)}{1+L(s)C_3(s)}, \tag{33}$$

with $L(s) = C_1(s)C_2(s)G(s)$. Using $(s - A_r)^{-1} = (R(s) - D_r)/(C_rB_r)$ we obtain

$$W = \frac{R(s) - D_r}{C_rB_r} \frac{1 - P(s)D_r}{1 - P(s)R(s)}. \tag{34}$$

For $Y = -Q_4^{-1}Q_3W$ we can write

$$Y = (sI - A - B_uD_rC_u)^{-1}B_uC_rW, \tag{35}$$

and again using the Lemma 3, we have

$$Y = (sI - A)^{-1}B_uC_rW - (sI - A)^{-1}B_u \left(\frac{D_r}{P(s)D_r - 1}\right) C_u(sI - A)^{-1}B_uC_rW. \tag{36}$$

Having $C_e(sI - A)^{-1}B_u = P(s)C_s(s)$, gives

$$\beta C_eY = \beta C_rW \frac{-P(s)C_s(s)}{P(s)D_r - 1}. \tag{37}$$

Finally, substituting (34) and (37) into (31) yields

$$H_\beta(s) = \beta'(R(s) - D_r)\frac{P(s)C_s(s)}{1 - P(s)R(s)} + \varrho'(R(s) - D_r)\frac{1 - P(s)D_r}{1 - P(s)R(s)}. \tag{38}$$

where $\beta' = -\beta/B_r$ and $\varrho' = \varrho/(C_rB_r)$ with $B_rC_r > 0$. Replacing $P(s)$ from (33) and simplifying yields

$$H_\beta(s) = \frac{\beta' L(s)C_s(s)\Big(R(s)-D_r\Big)+\varrho'\Big(1+L(s)(C_3(s)+D_r)\Big)\Big(R(s)-D_r\Big)}{1+L(s)(R(s)+C_3(s))}, \tag{39}$$

which is equal to the transfer function in (13). ■

APPENDIX C
PROOF OF THEOREM 2

According to Theorem 1, it is sufficient for quadratic stability of the RCS in (6) that $H_\beta(s)$ be SPR, $(\bar{A}, B_0)$ be controllable, $(\bar{A}, C_0)$ be observable, and $-1 \le \gamma \le 1$. The necessary SPR conditions for a $p \times p$ transfer function are given in Lemma 1. For the first condition in Lemma 1, $H_\beta(s)$ must satisfy the Hurwitz criterion. Since H_β and the base linear system share the same denominator, the expression in (13) implies that if both the base linear system and the shaping filter $C_s(s)$ are asymptotically stable (verifiable using standard LTI tools), this condition holds. Moreover, as $H_\beta(s)$ is a SISO transfer function, the second and third conditions in Lemma 1 correspond to steps 1 and 2, respectively. Step 3 examines controllability and observability of $(\bar{A}, B_0)$ and $(\bar{A}, C_0)$.

- Step 1: It is shown that there is a β and $\varrho > 0$ such that $\Re(H_\beta(j\omega)) > 0$ for all $\omega \in \mathbb{R}$.
- Step 2: It is shown that either $\lim_{s\to\infty} H_\beta(s) > 0$ or $\lim_{s\to\infty} H_\beta(s) = 0$ and $\lim_{\omega\to\infty} \omega^2\Re(H_\beta(j\omega)) > 0$.
- Step 3: It is shown that $(\bar{A}, B_0)$ and $(\bar{A}, C_0)$ are controllable and observable respectively.

Step 1: Since $H_\beta(s)$ is SISO, the frequency-domain part of the SPR condition reduces to requiring $\Re\{H_\beta(j\omega)\} > 0$ for all $\omega \in \mathbb{R}$. Using the representation in Lemma 4, this condition can be written as a positivity condition on the numerator after multiplication by the complex conjugate of the denominator. This step is the basis for introducing the Nyquist Stability Vector, since the real part of $H_\beta(j\omega)$ can be expressed as an inner product between the constant vector containing the free parameters β' and ϱ' and a frequency-dependent vector constructed from M_1, M_2, and M_3. It is first required to calculate the real part of $H_\beta(j\omega)$ in (13). Using the notations in (15), we have

$$H_\beta(j\omega) = \frac{\beta' M_2 + \varrho' M_3}{M_1}. \tag{40}$$

Multiplying both the numerator and the denominator by the complex conjugate of the denominator (M_1^*), yields

$$H_\beta(j\omega) = \frac{\beta' M_2M_1^* + \varrho' M_3M_1^*}{M_1M_1^*}, \tag{41}$$

where $\Re(M_1M_1^*) > 0$, and $I(M_1M_1^*) = 0$ ($I(.)$ means the imaginary part). Thus

$$\Re\Big(H_\beta(j\omega)\Big) = \frac{\beta'\Re\Big(M_2M_1^*\Big) + \varrho'\Re\Big(M_3M_1^*\Big)}{M_1M_1^*}. \tag{42}$$

To have $\Re\Big(H_\beta(j\omega)\Big) > 0$ it is needed to show that

$$\beta'\Re\Big(M_2M_1^*\Big) + \varrho'\Re\Big(M_3M_1^*\Big) > 0. \tag{43}$$

Considering $\vec{\mathcal{N}}(\omega)$ as (14), and defining $\vec{\xi} = \begin{bmatrix}\beta' & \varrho'\end{bmatrix}$, the equation (43) can be rewritten as

$$\vec{\xi}.\vec{\mathcal{N}}(\omega) > 0, \quad \forall\, \omega \in [0, \infty). \tag{44}$$

Having $\theta_\xi = \angle\vec{\xi}$, and $\theta_\mathcal{N}(\omega) = \angle\vec{\mathcal{N}}(\omega)$, (44) gives

$$|\vec{\xi}\,||\vec{\mathcal{N}}(\omega)|\cos\Big(\theta_\xi - \theta_\mathcal{N}(\omega)\Big) > 0, \ |\vec{\xi}\,| \neq 0, |\vec{\mathcal{N}}| \neq 0.$$

Thus, to have $\vec{\xi}.\vec{\mathcal{N}}(\omega) > 0$, we should have

$$\cos\Big(\theta_\xi - \theta_\mathcal{N}(\omega)\Big) > 0, \quad \forall\, \omega \in [0, \infty). \tag{45}$$

Since $\cos(x) > 0$ yields $-\frac{\pi}{2} < x < \frac{\pi}{2}$, we should have

$$-\frac{\pi}{2} < \theta_\xi - \theta_\mathcal{N}(\omega) < \frac{\pi}{2}, \quad \forall\omega \in [0, \infty). \tag{46}$$

Thus, knowing $-\infty < \beta' < \infty$ and $\varrho' > 0$, it gives

$$0 < \theta_\xi < \pi. \tag{47}$$

Let $\theta_1 = \min\theta_\mathcal{N}(\omega)$ and $\theta_2 = \max\theta_\mathcal{N}(\omega)$ (see Definition 2). In reference to (47), it follows that $(\theta_2 - \theta_1) < \pi$ must hold to satisfy (46). Furthermore, if $\theta_\mathcal{N}(\omega)$ lies in both intervals $[\pi, \frac{3\pi}{2})$ and $[-\frac{\pi}{2}, 0)$, it is evident that no $0 < \theta_\xi < \pi$ can satisfy (46).

Hence, (44) is satisfied if $(\theta_2 - \theta_1) < \pi$ and the phase of the Nyquist Stability Vector remains entirely within at least one of the following two admissible intervals:

- $-\frac{\pi}{2} < \theta_N(\omega) < \pi, \quad \forall\omega \in [0, \infty)$,
- $0 < \theta_N(\omega) < \frac{3\pi}{2}, \quad \forall\omega \in [0, \infty)$.

Step 2: Regarding the H_β transfer function in (13)

$$\lim_{s\to\infty} H_\beta(s) = \beta' L(s)C_s(s)\big(R(s) - D_r\big) + \varrho'\big(R(s) - D_r\big), \tag{48}$$

where, for both cases $\omega_r \neq 0$ and $\omega_r = 0$, it is required that either $\lim_{s\to\infty} H_\beta(s) > 0$, or $\lim_{s\to\infty} H_\beta(s) = 0$ and $\lim_{\omega\to\infty} \omega^2\Re\big(H_\beta(j\omega)\big) > 0$.

- $\omega_r \neq 0$ ($R(s) = \frac{\omega_k}{s+\omega_r} + D_r$)
  - $n-m = 1$ (the relative degree of $L(s)C_s(s)$)

$$\lim_{\omega\to\infty} \omega^2 \Re(H_\beta(j\omega)) = -\beta' K + \varrho' \omega_r \omega_k = \vec{\xi}\,.\vec{\mathcal{N}'},$$

by setting $\vec{\mathcal{N}'} = \begin{bmatrix} -K & \omega_r\omega_k \end{bmatrix}^T$, we have

$$\angle\vec{\mathcal{N}'} = \lim_{\omega\to\infty} \angle\vec{\mathcal{N}}(\omega) \overset{(17)}{\Longrightarrow} \theta_1 \leq \angle\vec{\mathcal{N}'} \leq \theta_2, \quad (49)$$

where, by using step 1, and starting from (44) for $\vec{\xi}\,.\vec{\mathcal{N}'}$, it gives: $\lim_{\omega\to\infty} \omega^2\Re(H_\beta(j\omega)) = \vec{\xi}\,.\vec{\mathcal{N}'} > 0$.

  - $n - m > 1$

$$\lim_{\omega\to\infty} \omega^2 \Re(H_\beta(j\omega)) = \varrho' \omega_r \omega_k > 0. \quad (50)$$

- $\omega_r = 0$
  - $n - m > 1$

$$\lim_{\omega\to\infty} \omega^2 \Re(H_\beta(j\omega)) = 0, \quad (51)$$

This implies that $H(j\omega)$ is not SPR when $n-m > 1$.

  - $n-m = 1$

$$\lim_{\omega\to\infty} \omega^2 \Re(H_\beta(j\omega)) = -\beta' \frac{K_n}{K_m} > 0, \quad (52)$$

means that in this case, the relative degree can only be 1, and $-\beta' \frac{K_n}{K_m} > 0$. Regarding the transfer function in (18), for $n - m = 1$ we have $L(\infty)C_s(\infty) = \frac{K_n}{K_m s}$. Which leads to the following conditions:

- The relative degree of the transfer function $L(s)C_s(s) = C_1(s)C_2(s)G(s)C_s(s)$ must be 1.
- If $\lim_{s\to\infty} \angle(L(s)C_s(s)) = -\pi/2$ ($\frac{K_n}{K_m} > 0$), then $0 < \theta_{\mathcal{N}}(\omega) < \frac{3\pi}{2}$.
- If $\lim_{s\to\infty} \angle(L(s)C_s(s)) = -3\pi/2$ ($\frac{K_n}{K_m} < 0$), then $-\frac{\pi}{2} < \theta_{\mathcal{N}}(\omega) < \pi$.

Step 3: The role of this step is to exclude pole-zero cancellations in the realization of $H_\beta(s)$ associated with $(\bar{A}, B_0, C_0)$. If the numerator and denominator of $H_\beta(s)$ do not have a common root, then the corresponding realization is minimal, and hence the pairs $(\bar{A}, B_0)$ and $(\bar{A}, C_0)$ are controllable and observable, respectively. Therefore, it is sufficient to show that the admissible choice of β' and ϱ' can be made such that the numerator $\beta' M_2 + \varrho' M_3$ does not vanish at the roots of the denominator M_1. Let $a_0 + jb_0$ be a root of the denominator. Then considering the $H_\beta(s) = \frac{\beta' M_2 + \varrho' M_3}{M_1}$ in (40), with $M_1(a_0, b_0) = 0$, where the numerator must not have any root at $a_0 + jb_0$, which means

$$\beta' M_2(a_0, b_0) + \varrho' M_3(a_0, b_0) \neq 0. \quad (53)$$

Here we assume there is a pair of (β_1', ϱ_1') such that

$$\beta_1' M_2(a_0, b_0) + \varrho_1' M_3(a_0, b_0) = 0. \quad (54)$$

First, we consider the case that $M_2(a_0, b_0) \neq 0$, and/or $M_3(a_0, b_0) \neq 0$. From Step 1, the admissible choices of β' and ϱ' are those for which the angle θ_ξ of the vector $\vec{\xi} = [\beta' \ \varrho']^\top$ satisfies

$$\theta_\xi \in \left(\theta_2 - \frac{\pi}{2}, \theta_1 + \frac{\pi}{2}\right).$$

Since $(\theta_2 - \theta_1) < \pi$, this interval is nonempty. Therefore, for a sufficiently small $\epsilon > 0$, a new pair $(\beta_2', \varrho_1') = (\beta_1' + \epsilon, \varrho_1')$ can be selected such that the corresponding angle remains in the admissible interval. Substituting the new pairs in (54) yields,

$$\begin{aligned} &\beta_2' M_2(a_0, b_0) + \varrho_1' M_3(a_0, b_0) \\ &= (\beta_1' + \varepsilon) M_2(a_0, b_0) + \varrho_1' M_3(a_0, b_0) \\ &= \beta_1' M_2(a_0, b_0) + \varrho_1' M_3(a_0, b_0) + \varepsilon M_2(a_0, b_0) \\ &= \varepsilon M_2(a_0, b_0) \neq 0. \end{aligned} \quad (55)$$

Thus, for the case that $M_2(a_0, b_0) \neq 0$, and/or $M_3(a_0, b_0) \neq 0$, it is possible to find a pair (β', ϱ') such that $H_\beta(s)$ be SPR and does not have any pole-zero cancellation. Now for the case $M_2(a_0, b_0) = M_3(a_0, b_0) = M_1(a_0, b_0) = 0$, if we show that when $M_1(a_0, b_0) = 0$, always one of the transfer functions $M_2(a_0, b_0)$ or $M_3(a_0, b_0)$ is non-zero, then there is no pole-zero cancellation, and the proof is done. Thus, consider

$$M_1(a_0, b_0) = 1 + L(a_0, b_0)\Big(C_3(a_0, b_0) + R(a_0, b_0)\Big) = 0, \quad (56)$$

$$\begin{aligned} M_3(a_0, b_0) = &\Big(1 + L(a_0, b_0)\Big(C_3(a_0, b_0) + D_r\Big)\Big) \\ &\ldots \Big(R(a_0, b_0) - D_r\Big) = 0, \end{aligned} \quad (57)$$

(57) yields three cases,

$$\text{I}: \begin{cases} 1 + L(a_0, b_0)\Big(C_3(a_0, b_0) + D_r\Big) = 0, \\ R(a_0, b_0) - D_r \neq 0, \end{cases} \quad (58)$$

$$\text{II}: \begin{cases} 1 + L(a_0, b_0)\Big(C_3(a_0, b_0) + D_r\Big) \neq 0, \\ R(a_0, b_0) - D_r = 0, \end{cases} \quad (59)$$

$$\text{III}: \begin{cases} 1 + L(a_0, b_0)\Big(C_3(a_0, b_0) + D_r\Big) = 0, \\ R(a_0, b_0) - D_r = 0. \end{cases} \quad (60)$$

For the case I, we have $1 + L(a_0, b_0)\Big(C_3(a_0, b_0) + D_r\Big) = 0$, where regarding M_1 in (56), it yields $R(a_0, b_0) = D_r$, which is not possible to have $R(a_0, b_0) - D_r = 0$ in case I. For cases II and III, $R(a_0, b_0) - D_r = 0$, implying $\frac{\omega_k}{s+\omega_r} + D_r = D_r$, where $\frac{\omega_k}{s+\omega_r}$ can not be zero ($\omega_k > 0$). Thus, it is also not possible to have $M_3(a_0, b_0) = 0$ and $M_1(a_0, b_0) = 0$ in these cases. Consequently, there is no pole-zero cancellation, and the pairs $(\bar{A}, C_0)$ and $(\bar{A}, B_0)$ are observable and controllable, respectively. ■

ACKNOWLEDGMENT

The authors sincerely appreciate the invaluable collaboration, insightful contributions, and generous support of Luke F. van Eijk and Dragan Kostić from ASMPT throughout this project.

REFERENCES

[1] G. Zhao, D. Nešić, Y. Tan, and C. Hua, "Overcoming overshoot performance limitations of linear systems with reset control," *Automatica*, vol. 101, pp. 27–35, Mar. 2019.

[2] J. C. Clegg, "A nonlinear integrator for servomechanisms," *Trans. Amer. Inst. Electr. Eng., II, Appl. Ind.*, vol. 77, no. 1, pp. 41–42, Mar. 1958.

[3] Y. Guo, Y. Wang, and L. Xie, "Frequency-domain properties of reset systems with application in hard-disk-drive systems," *IEEE Trans. Control Syst. Technol.*, vol. 17, no. 6, pp. 1446–1453, Nov. 2009.
[4] L. Zaccarian, D. Nesic, and A. R. Teel, "First order reset elements and the clegg integrator revisited," in *Proc. Amer. Control Conf.*, 2005, pp. 563–568.
[5] D. Nešić, A. R. Teel, and L. Zaccarian, "Stability and performance of SISO control systems with first-order reset elements," *IEEE Trans. Autom. Control*, vol. 56, no. 11, pp. 2567–2582, Nov. 2011.
[6] N. Saikumar, K. Heinen, and S. H. HosseinNia, "Loop-shaping for reset control systems: A higher-order sinusoidal-input describing functions approach," *Control Eng. Pract.*, vol. 111, 2021, Art. no. 104808.
[7] S. J. L. M. van Loon, K. G. J. Gruntjens, M. F. Heertjes, N. van de Wouw, and W. P. M. H. Heemels, "Frequency-domain tools for stability analysis of reset control systems," *Automatica*, vol. 82, pp. 101–108, Aug. 2017.
[8] S. van den Eijnden, T. Chaffey, T. Oomen, and W. P. M. H. M. Heemels, "Scaled graphs for reset control system analysis," *Eur. J. Control*, vol. 80, Nov. 2024, Art. no. 101050.
[9] O. Beker, C. V. Hollot, Y. Chait, and H. Han, "Fundamental properties of reset control systems," *Automatica*, vol. 40, no. 6, pp. 905–915, Jun. 2004.
[10] Y. Guo, L. Xie, and Y. Wang, *Analysis and Design of Reset Control Systems*. London, U.K.: IET, 2015.
[11] A. Baños and A. Barreiro, *Reset Control Systems*, 1st ed., London, U.K.: Springer, 2012.
[12] A. A. Dastjerdi, A. Astolfi, and S. H. HosseinNia, "Frequency-domain stability methods for reset control systems," *Automatica*, vol. 148, Feb. 2023, Art. no. 110737.
[13] A. A. Dastjerdi, A. Astolfi, N. Saikumar, N. Karbasizadeh, D. Valério, and S. H. HosseinNia, "Closed-loop frequency analysis of reset control systems," *IEEE Trans. Autom. Control*, vol. 68, no. 2, pp. 1146–1153, Feb. 2023.
[14] S. A. Hosseini, F. R. Quinten, L. F. van Eijk, D. Kostic, and S. H. HosseinNia, "Frequency-domain design of a reset-based filter: An add-on nonlinear filter for industrial motion control," *IEEE Trans. Control Syst. Technol.*, vol. 34, no. 2, pp. 919–933, Feb. 2026.
[15] L. F. van Eijk, Y. Liu, X. Zhang, D. Kostić, and S. H. HosseinNia, "A nonlinear integrator based on the first-order reset element," *IFAC-PapersOnLine*, vol. 58, no. 7, pp. 382–387, 2024.
[16] L. F. van Eijk, D. Kostić, and S. H. HosseinNia, "Frequency response analysis of general zero-crossing reset control systems," *IEEE Control Syst. Lett.*, vol. 9, pp. 1105–1110, 2025.
[17] D. Nešić, L. Zaccarian, and A. R. Teel, "Stability properties of reset systems," *Automatica*, vol. 44, no. 8, pp. 2019–2026, Aug. 2008.
[18] H. K. Khalil, *Nonlinear Systems*, 3rd ed., Upper Saddle River, NJ, USA: Prentice-Hall, 2002.
[19] A. Pavlov, N. van de Wouw, and H. Nijmeijer, "Frequency response functions for nonlinear convergent systems," *IEEE Trans. Autom. Control*, vol. 52, no. 6, pp. 1159–1165, Jun. 2007.
[20] H. L. Trentelman, A. A. Stoorvogel, and M. Hautus, *Control Theory for Linear Systems*. London, U.K.: Springer, 2001.
[21] N. J. Higham, *Accuracy and Stability of Numerical Algorithms*, 2nd ed., Philadelphia, PA, USA: SIAM, 2002.
[22] A. Rantzer, "On the Kalman–Yakubovich–Popov lemma," *Syst. Control Lett.*, vol. 28, no. 1, pp. 7–10, 1996.
[23] R. A. Horn and C. R. Johnson, *Matrix Analysis*, 2nd ed. Cambridge, U.K.: Cambridge Univ. Press, 2012.

ALI HOSSEINI received the M.Sc. degree in systems and control engineering from Sharif University of Technology, Tehran, Iran, in 2022, specializing in nonlinear control (with a focus on hybrid integrator-gain systems). He is currently pursuing the Ph.D. degree with the Department of Precision and Microsystems Engineering, Delft University of Technology, Delft, The Netherlands.

His research focuses on addressing industrial control challenges using nonlinear control techniques in close collaboration with ASMPT, Beuningen, The Netherlands. His research interests include precision motion control, nonlinear control systems, such as reset and hybrid systems, and mechatronic system design.

HASSAN HOSSEINNIA (Senior Member, IEEE) received the Ph.D. degree (cum laude) in electrical engineering, in 2013, with a specialization in automatic control and its applications in mechatronics.

He is currently a Faculty Member with Delft University of Technology (TU Delft), where he leads advanced research in precision mechatronic system design, high-performance motion control, active vibration damping, and the development of electromagnetic and piezoelectric actuators. His work has gained international recognition. In 2024, he received the Abel Young Scientists Award at the 12th IFAC Conference on Fractional Differentiation and its Applications. His current research focuses on developing innovative control strategies and system architectures to improve bandwidth and precision in next-generation mechatronic systems.

Dr. HosseinNia is a member of the editorial boards of leading journals, including *Mechatronics*, *Control Engineering Practice*, and *Fractional Calculus and Applied Analysis*. He has also contributed significantly to the academic community. He served as the General Chair for the 7th IEEE International Conference on Control, Mechatronics, and Automation (ICCMA 2019). Through his work, he combines strong theoretical expertise with real-world industrial applications, driving innovation in advanced control and mechatronic system design.